Liquid Crystals
Publication details, including instructions for authors and subscription information:
http://www.informaworld.com/smpp/title~content=t713926090

Electroclinic effect in the chiral smectic A and cholesteric phases at the proximity of a N*-SmA-SmC* multicritical point

J. Hemine[abc]; A. Daoudi[bc]; C. Legrand[bd]; A. El Kaaouachi[e]; A. Nafidi[e]; H. T. Nguyen[f]
[a] Université Hassan II Mohammedia-Casablanca, Mohammedia, Maroc [b] Université Lille Nord de France, Lille, France [c] ULCO, UDSMM, Dunkerque, France [d] ULCO, UDSMM, Calais, France [e] LPMC, Faculté des Sciences Ibnou Zohr, Agadir, Maroc [f] CRPP, Université de Bordeaux 1, Pessac, France

Online publication date: 20 October 2010

To cite this Article Hemine, J. , Daoudi, A. , Legrand, C. , El Kaaouachi, A. , Nafidi, A. and Nguyen, H. T.(2010) 'Electroclinic effect in the chiral smectic A and cholesteric phases at the proximity of a N*-SmA-SmC* multicritical point', Liquid Crystals, 37: 10, 1313 — 1319
To link to this Article: DOI: 10.1080/02678292.2010.504864
URL: http://dx.doi.org/10.1080/02678292.2010.504864

Liquid Crystals,
Vol. 37, No. 10, October 2010, 1313–1319

Taylor & Francis
Taylor & Francis Group

Electroclinic effect in the chiral smectic A and cholesteric phases at the proximity of a N*–SmA–SmC* multicritical point

J. Hemine[a,b,c]*, A. Daoudi[b,c], C. Legrand[b,d], A. El Kaaouachi[e], A. Nafidi[e] and H.T. Nguyen[f]

[a]*Université Hassan II Mohammedia-Casablanca, Mohammedia, Maroc;* [b]*Université Lille Nord de France, Lille, France;* [c]*ULCO, UDSMM, Dunkerque, France;* [d]*ULCO, UDSMM, Calais, France;* [e]*LPMC, Faculté des Sciences Ibnou Zohr, Agadir, Maroc;* [f]*CRPP, Université de Bordeaux 1, Pessac, France*

(*Received 22 June 2010; final version received 25 June 2010*)

We studied the electro-optic and dielectric properties of three pure ferroelectric liquid crystal materials (C10, C11 and C12) of the same series exhibiting cholesteric (N*), smectic A (SmA) and chiral smectic C (SmC*) phases. From electro-optic investigations, the tilt angle and spontaneous polarisation were determined as a function of temperature. In the dielectric measurements carried out without a dc bias field, we studied the soft-mode relaxation in the SmA phase. From experimental data and using the results of a Landau model, we evaluated the soft-mode rotational viscosity and the electroclinic coefficient in the SmA phase. A soft-mode like mechanism was also observed in the N* phase for compounds with shorter chains (C10 and C11). This relaxation process is not detected for the homologue with a longer chain (C12). The observation of this mechanism is related to smectic order fluctuations within N* phase whose amplitude is increased when approaching the SmC*–SmA–N* multicritical point.

Keywords: liquid crystal materials; ferroelectricity; dielectric loss and relaxation; electro-optic study

1. Introduction

The electroclinic effect in ferroelectric liquid crystals (FLCs) has attracted increasing interest over the past decades because of their potential applications mainly in electro-optic devices as linear light modulators with a fast response time. The electroclinic effect, which is a switching mechanism that exists around the chiral smectic C (SmC*) to smectic A (SmA) transition, was first demonstrated by Garoff and Meyer [1, 2] and corresponds to an induced tilt of long molecular axes when an electric field is applied parallel to the smectic planes.

The electroclinic effect was described by a phenomenological model derived from the Landau theory which predicts a linear dependence of the induced tilt angle on the applied field [3]. Marcerou [4] extended Meyer's theory of the electroclinic effect and showed that the trilinear coupling between the smectic layers, the tilt angle and the electric polarisation is responsible for the electroclinic effect in the SmC*, SmA and cholesteric (N*) phases, especially in the proximity of an N*–SmA–SmC* multicritical point.

For materials exhibiting the N*–SmA–SmC* phase sequence [5–7], the electroclinic effect generally observed in the SmA phase [8–12] near to the SmA-SmC* phase transition can be also detected in the N* phase [13–16] around the N*–SmA [7, 17, 18] or N*–SmC* [7, 12, 13, 16, 19] transitions. Furthermore, for biphenyl alkyloxy benzoate materials [20] (Table 1) which exhibit high polarisations, the electroclinic effect amplitude was demonstrated to be important near to the SmC*–SmA and SmA–N* phase transitions. In a previous paper [21], we observed by dielectric spectroscopy a relaxation process in the N* phase. We interpreted this relaxation mechanism as an electroclinic effect analogous to that classically observed in the SmA phase.

In this paper, we show that the dielectric relaxation process observed in the N* phase for C10 and C11 disappears for the C12 compound. For this purpose, we performed an experimental characterisation of the three materials including electro-optic and dielectric investigations. The temperature dependences of the tilt angle and spontaneous polarisation in the SmC* phase were studied. Using the dielectric spectroscopy without a dc bias field, we investigated the relaxation mechanisms related to ferroelectricity and/or smectic orders. The relaxation frequency and dielectric strength of these mechanisms in the SmA phase were measured as a function of temperature near to the SmC*–SmA and SmA–N* transition temperatures.

2. Experimental

In this study we used three pure FLC compounds (C10, C11 and C12) of the homologous biphenyl alkyloxy benzoate series, which are present on heating the following phase sequence between the crystalline and the isotropic phases: chiral smectic C–smectic A– cholesteric–blue phase (SmC*–SmA–N*–BP).

*Corresponding author. Email: jamal.hemine@yahoo.fr
[a]Permanent address

ISSN 0267-8292 print/ISSN 1366-5855 online

DOI: 10.1080/02678292.2010.504864
http://www.informaworld.com

Table 1. Chemical formulae, phase sequences and transition temperatures (°C) for the homologues of the biphenyl benzoate series.

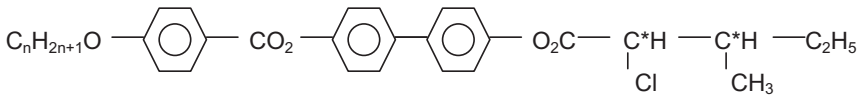

n	Cr	Sm	SmC*	SmA	N*	BP	I
7	• 100	• (52)	• 134	–	• 166	• 166.1	•
8	• 88	–	• 138	–	• 165.5	• 166.5	•
9	• 89	–	• 142	–	• 162	• 162.1	•
10	• 88	–	• 143	• 144	• 159	• 160	•
11	• 88	–	• 146	• 149	• 157	• 157.1	•
12	• 81	–	• 145.5	• 150	• 154	• 154.5	•

Notes: Cr: crystalline phase; Sm: smectic phases A, C*; N*: cholesteric phase; BP: blue phase; I: isotropic phase; •: phase exists; –:phase does not exist; ( ): monotropic transition.

The chemical structure, phase sequences and transition temperatures at atmospheric pressure determined both by polarised optical microscopy and differential scanning calorimetry are summarised in Table 1. It can be seen from this table that the first three compounds of the series (C7–C9) do not exhibit the SmA phase. The temperature range of the SmA phase increases from 1°C, 3°C and 4.5°C for C10, C11 and C12, respectively (see Table 1). The N*–SmA–SmC* multicritical point is approached as the length of the alkyloxy chain decreases. For this reason, we focused our experimental studies on the C12 compound as we suspected that the relaxation process observed near a multicritical point for C10 and C11 derivatives disappears completely for C12 far from this multicritical point.

The tilt angle, θ, and spontaneous polarisation, P_s, were measured as a function of temperature by using the surface-stabilised ferroelectric liquid crystal (SSFLC) configuration [22]. For these studies, a 3 μm thick cell coated with ITO (indium tin oxide) and rubbed polyimide was used to promote a planar geometry. A classical electro-optic setup was used for the measurements of θ [23] and P_s [24]. The tilt angle measurements were performed by applying a 0.2 Hz square wave voltage at 5 V μm^{-1} electric field amplitude. To measure P_s, a 1 kHz triangular wave of 5 V μm^{-1} amplitude was used.

The measurements of the complex permittivity were carried out in the frequency range of 5 Hz to 1 MHz on planar geometry with smectic layers perpendicular to the electrodes (bookshelf geometry) using a previously described experimental procedure [25]. To obtain a good alignment, the sample was inserted in the cell by capillarity action in the isotropic phase. To check the textures and transition temperatures, the samples were observed by means of a polarised optical microscope between crossed polarisers. The electric field was applied perpendicular to the helical axis of the SmC* structure and parallel to the smectic layers. The measurements were made without superimposition of a dc bias field on the measuring electric field. The dielectric relaxation mechanisms related to the ferroelectric properties were determined by fitting the complex permittivity $\varepsilon^*(\omega,T) = \varepsilon' - j\varepsilon''$ for which the Cole–Cole distribution [26] type may be written as

$$\varepsilon^*(\omega,T) = \varepsilon_\infty + \frac{\Delta\varepsilon_G}{1+(j\omega\tau_G)^{1-\alpha_G}} + \frac{\Delta\varepsilon_S}{1+(j\omega\tau_S)^{1-\alpha_S}} + \frac{\sigma}{j\omega\varepsilon_0} \quad (1)$$

where: $\Delta\varepsilon_G$ and $\Delta\varepsilon_S$ correspond to the dielectric strengths due to the orientation polarisations of the Goldstone and soft modes, respectively; $\tau_G = 1/2\pi f_G$ and $\tau_S = 1/2\pi f_S$ correspond, respectively, to their relaxation times; ε_∞ represents the limit of the dielectric permittivity at high frequency range; σ and ω are the static conductivity and angular frequency of the applied electric field, respectively; and α_i and f_i are, respectively, the corresponding distribution parameter and relaxation frequency of the relaxation mode i (i = Goldstone or soft mode).

The real part ε' of the complex permittivity is the usual dielectric constant, while the imaginary part ε'' accounts for dielectric losses. The dielectric soft-mode measurements with a dc bias field in the SmC* and SmA phases, as well as the electroclinic effect in the N* phase around the SmC*–SmA–N* multicritical point on C10, C11 and C12 compounds, were reported in previous papers [21, 27].

3. Results and discussion

3.1 *Electro-optic properties*

The temperature dependence of the tilt angle (θ) for C10, C11 and C12 materials is shown in Figure 1. At

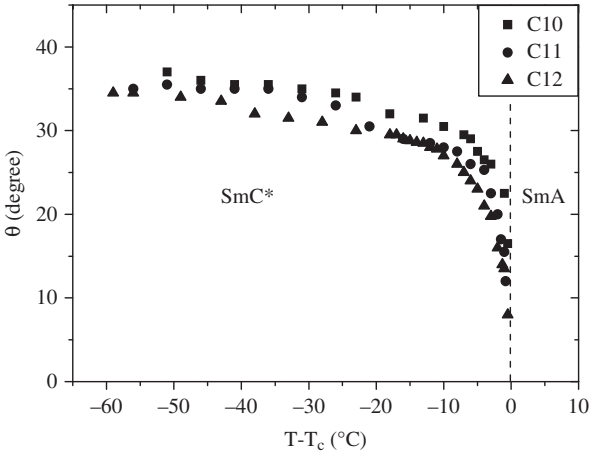

Figure 1. Tilt angle θ temperature dependence for C10, C11 and C12.

low temperatures and far from T_C, θ reaches the saturation value of 35°. With increasing temperature, θ rapidly decreases close to T_C. As the temperature increases, θ decreases continuously up to the SmC*–SmA transition temperature (T_C), where it is about 16°, 12° and 8° for C10, C11 and C12, respectively. This apparent tilt angle at T_C had already been observed for many compounds [8] and is due to the electroclinic effect, i.e. to the coupling between the applied electric field and the molecular director.

Figure 2 shows our plot of a typical example of spontaneous polarisation measurements versus temperature. As can be seen from this figure, high values of P_S were measured: $P_S = 160$, 140 and 120 nC cm^{-2} for C10, C11 and C12, respectively. The high values of P_s obtained for these compounds are principally due to the presence of the ester group (–COO-) which links the chiral alkyloxy chain to the biphenyl core near to an electron-attracting Cl atom. Therefore, decreasing the alkyloxy chain length in this series results in an increase

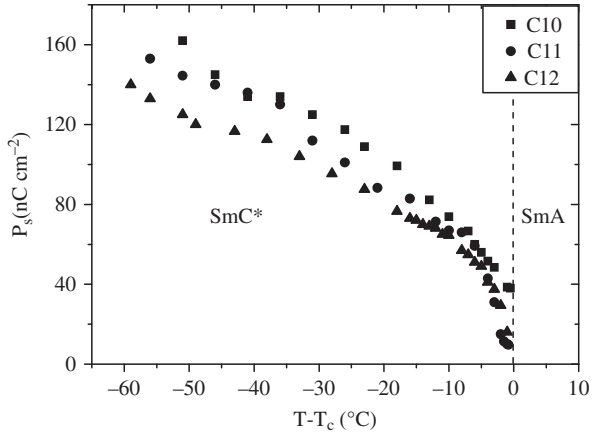

Figure 2. Spontaneous polarisation P_s temperature dependence for C10, C11 and C12.

in ferroelectric polarisation. This effect can be explained by the fact that, for the C12 compound, the longer alkyloxy chain prevents a rotational motion of the molecules [5] compared to C10 and C11, leading to a reduction in the amplitude of the spontaneous polarisation.

3.2 Dielectric responses

For C10, C11 and C12 compounds, the dielectric spectra without a dc bias field in the SmA phase display one relaxation mechanism at higher frequencies. The dielectric strength of this mechanism increases as the temperature T_C is approached from the SmA phase. This is why this mechanism was attributed to the soft-mode relaxation. We also detected another relaxation process at higher frequencies in the N* phase for C10 and C11 materials.

The temperature dependences of the soft-mode dielectric strength, $\Delta\varepsilon_S$, and the corresponding relaxation frequency, f_S, in the SmA phase are depicted in Figures 3, 4 and 5 for C10, C11 and C12, respectively.

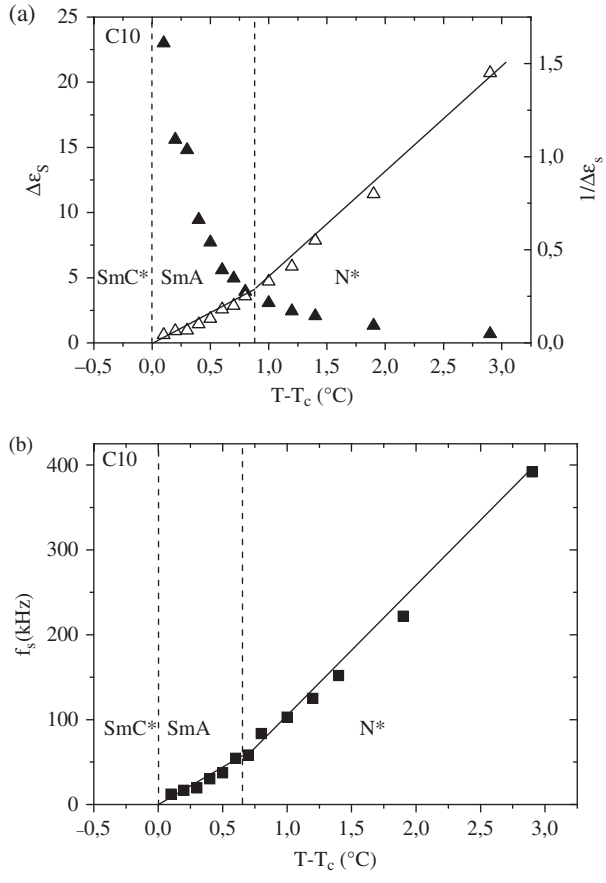

Figure 3. Dielectric strength (a) and relaxation frequency (b) of the soft-mode in the SmA phase and of the relaxation mechanism observed in the N* phase versus temperature for C10. The reciprocal dielectric strength $1/\Delta\varepsilon_S$ (open symbol) is also reported (a).

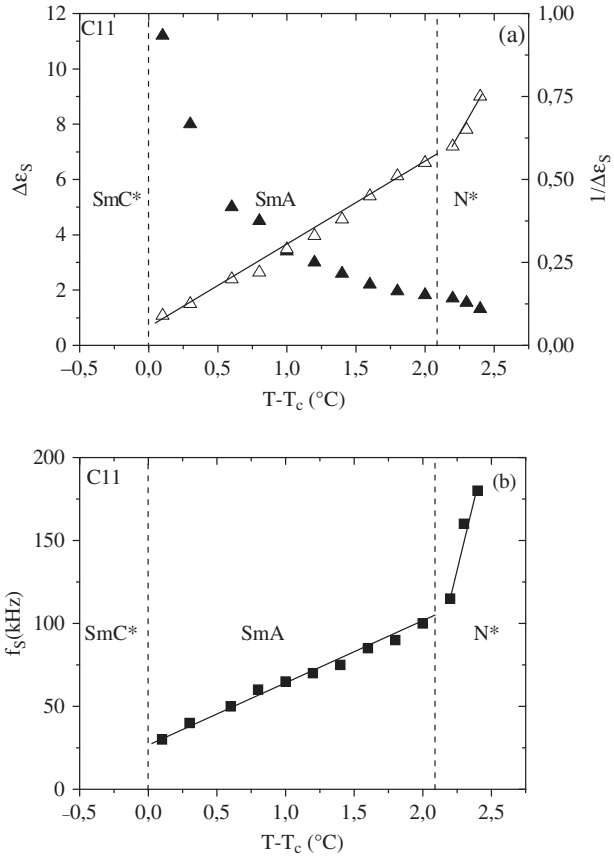

Figure 4. Dielectric strength (a) and relaxation frequency (b) of the soft-mode in the SmA phase and of the relaxation mechanism observed in the N* phase versus temperature for C11. The reciprocal dielectric strength $1/\Delta\varepsilon_S$ (open symbol) is also reported (a).

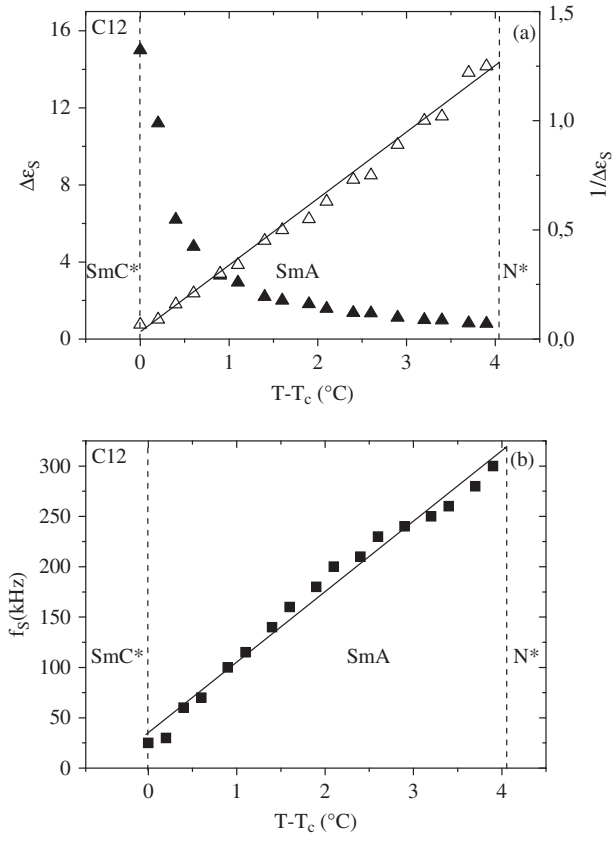

Figure 5. Dielectric strength (a) and relaxation frequency (b) of the soft-mode in the SmA phase and of the relaxation mechanism observed in the N* phase versus temperature for C12. The reciprocal dielectric strength $1/\Delta\varepsilon_S$ (open symbol) is also reported (a).

The reciprocal dielectric strength ($1/\Delta\varepsilon_S$) and f_S linearly depend on T-T_C (see Figures 3, 4 and 5). Such behaviour agrees with the theoretical model [28] which predicts that close to T_C, $1/\Delta\varepsilon_S$ and f_S satisfy the Curie–Weiss law. The $\Delta\varepsilon_S$ values vary far from T_C to $T = T_C$ from 4 to 23 for C10, 2 to 11 for C11 and from 0.7 to 15 for C12, whereas the temperature dependence of f_S in the SmA varies in the range 45–6 kHz for C10, 100–25 kHz for C11 and 325–25 kHz for C12. For C10 and C11, the same behaviour is observed in the N* phase near to the N*–SmA transition with continuity of the characteristic parameters. Indeed, in the N* phase there are linear evolutions of both the inverse of the amplitude, $1/\Delta\varepsilon_S(T)$, and the relaxation frequency, $f_S(T)$. The continuation of the characteristic parameters from the SmA to the N* phase is marked by abrupt changes of slope values (see Table 2 and Figures 3 and 4). However, unlike the C10 and C11 homologues, we did not observe any relaxation mechanism in the high frequency range in the N* phase of C12.

Table 2. Experimental slope values for the reciprocal dielectric strength and the relaxation frequency in the SmA and N* phases for C10, C11 and C12.

Compound	$[d(1/\Delta\varepsilon_S)/dT]_{SmA}$ (/°C)	$[d(1/\Delta\varepsilon_S)/dT]_{N^*}$ (/°C)	$[d(f_S)/dT]_{SmA}$ (kHz/°C)	$[d(f_S)/dT]_{N^*}$ (kHz/°C)
C10	0.30	0.55	70	150
C11	0.25	0.75	35	320
C12	0.30	–	72	–

3.3 Electroclinic effect

From electro-optic and dielectric data, and using the predictions of generalised Landau models [28, 29], we can determine some characteristic parameters of the soft mode in the SmA phase. The dielectric strength and the relaxation frequency of the soft mode in the paraelectric SmA phase are given by

$$\varepsilon_0 \Delta\varepsilon_{SA} = \frac{(\chi C)^2}{K_{33}q^2 + \alpha(T - T_C)}, \quad (2)$$

$$f_{SA} = \frac{K_{33}q^2 + \alpha(T - T_C)}{2\pi\gamma_{SA}}, \quad (3)$$

where: K_{33} is the twist elastic constant; α is the mean-field coefficient; $q = 2\pi/p$ is the wave vector of the modulated SmC* phase; χ is the electric susceptibility of the FLC; ε_0 is the permittivity of free space; and γ_{SA} is the soft-mode rotational viscosity in the SmA phase. C is related to the piezoelectric bilinear coupling between the tilt and polarisation according to

$$P_S \cong (\chi C)\theta. \quad (4)$$

As we can see from Equations (2) and (3), the reciprocal dielectric strength, $1/(\varepsilon_0\Delta\varepsilon_{SA}) \cong \alpha(T - T_C)/\chi^2C^2$, and the relaxation frequency, $f_{SA} \cong \alpha(T - T_C)/2\pi\gamma_{SA}$, in the SmA phase decrease linearly with temperature when approaching T_C. The elastic term ($K_{33}q^2$) was reasonably neglected here because the dielectric response close to T_C is principally governed by the thermal term [$\alpha(T–T_C)$]. The value of γ_{SA} can be calculated from

$$\gamma_{SA} = \frac{\left(P_s/\theta\right)^2}{2\pi\varepsilon_0} \frac{\left(d\Delta\varepsilon_s^{-1}/dT\right)}{\left(df_s/dT\right)}. \quad (5)$$

According to the experimental values depicted in Table 2, the values of the soft-mode rotational viscosity were determined in the SmA phase close to T_C. We obtained $\gamma_{SA} = 75$ mPa s for C10; a value of $\gamma_{SA} = 37$ mPa s is found for C11 and C12. The latter value of γ_{SA} is two times lower than that obtained for C10. These values are in the same order of magnitude of those measured in the SmA phase by other authors [10, 30] for many other FLC compounds.

We now determine the electroclinic coefficient, e_C, in the SmA phase close to T_C. The temperature dependence of e_C is expressed in the following equation [1, 28]:

$$e_C = \frac{\varepsilon_0\Delta\varepsilon_{SA}}{\chi C} \cong \frac{\varepsilon_0\chi C}{\alpha(T - T_C)}. \quad (6)$$

Figures 6(a), 6(b) and 6(c) give the temperature evolution of e_C in the SmA phase for C10, C11 and C12, respectively. For all studied compounds, the electroclinic coefficient $e_C(T–T_C)$ is characterised by a rapid decrease near to T_C when T increases, followed by a slow decrease when going towards the N* phase. For C10, we obtained at $T \cong T_C$ a large value of

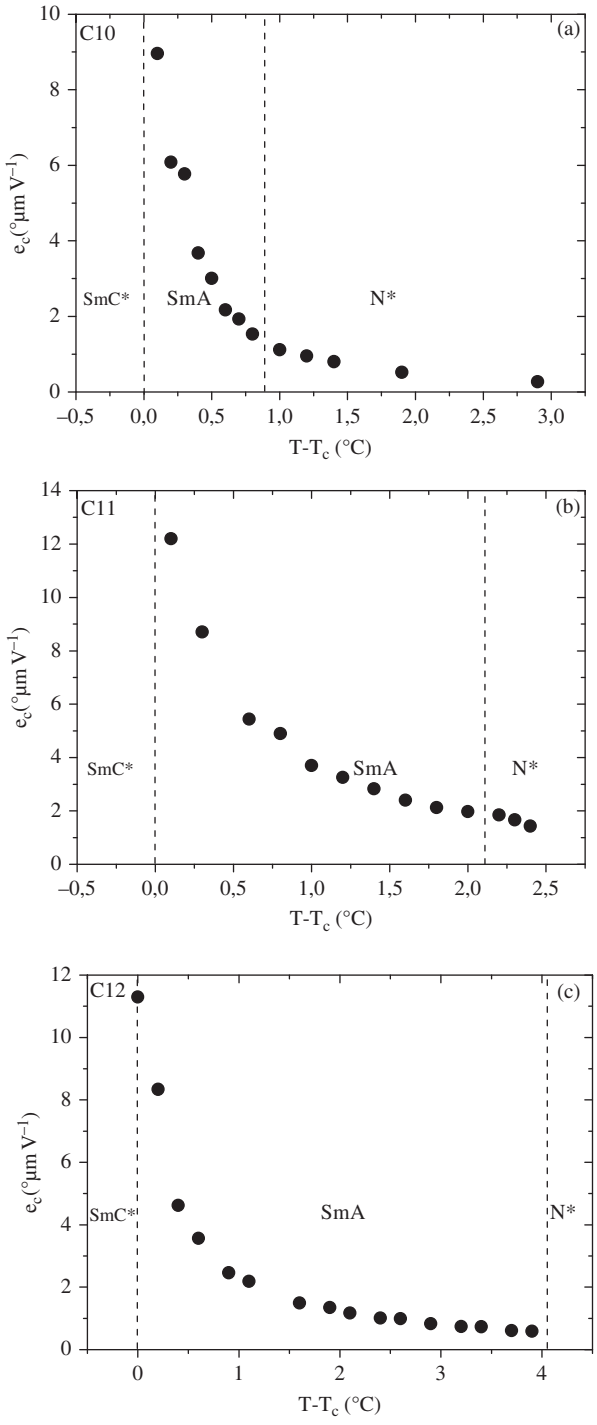

Figure 6. Temperature dependence of the electroclinic coefficient e_C of the soft-mode in the SmA phase and of the mechanism observed in the N* phase for C10 (a), C11 (b) and C12 (c).

e_C~9°µm V^{-1}, which decreased to ~2°µm V^{-1} near to the SmA–N* transition. For C11 and C12, this electroclinic coefficient increased up to e_C~12 °µm V^{-1} at T_C. This value obtained in the SmA just above the

SmA–SmC* transition is comparable with that obtained by Petit *et al.* [30] for a commercial FLC material, and with values reported by Bahr and Heppke [8] for a FLC material with a high spontaneous polarisation ($P_S \approx 150$ nC cm^{-2}). The magnitude of the electroclinic coefficient is proportional to the piezoelectric coupling term χC [Equation (6)], which is related to the spontaneous polarisation [Equation (4)]. For our materials, which have high polarisations ($P_S \approx 160$, 140 and 120 nC cm^{-2} for C10, C11 and C12, respectively), the values of e_C are important especially near to the SmC*–SmA and SmA–N* transitions.

On the other hand, for C10 and C11 materials, a similar value of $e_C \sim 2°\mu m\ V^{-1}$ was obtained at the SmA–N* transition. The relaxation process detected in the N* phase is in perfect continuity with the soft mode observed in the SmA phase (Figures 6(a) and 6(b)). This mechanism can thus be attributed to a soft-mode like relaxation in the N* phase. The transition from SmA to N* phase was picked out by changes on $d(1/\Delta\varepsilon_S)/dT$ and df_s/dT slopes (Figures 3 and 4). The great difference in the slope values confirms that the relaxation process observed in the SmA phase is still detected in the N* phase. The electroclinic effect in the N* phase had already been observed and reported [7, 13, 17]. The values of e_C found here are much larger than those reported by Extebarria *et al.* [7], Komitov *et al.* [13] and Li *et al.* [17], who studied the electroclinic effect in a fairly long helical pitch (> 30 μm) N* phase of FLC mixtures near to the SmA–N* transition. It is worth mentioning that the dielectric mechanism detected and studied here without a dc bias field in the N* phase for C10 and C11 materials was also observed under a dc bias field of 1 V μm^{-1} [21].

In our early studies [20, 21], we demonstrated that the relaxation process observed in the N* phase has the same behaviour as the soft mode classically observed in the SmA phase. We have explained this effect by the existence of local fluctuations of smectic order [13, 16, 31], namely cybotactic groups [13] within N* phase. These fluctuations are emphasised because of the proximity of the N*–SmA–SmC* multicritical point where the thermodynamic conditions are favourable to the appearance of a large fluctuation of the orthogonal smectic order. The relaxation process observed in the N* phase persists only in a narrow temperature range in the vicinity of the SmA–N* transition (2°C and 0.3°C above the SmA–N* transition, respectively for C10 and C11); whereas the temperature domain of N* phase is about 13°C for C10 and 8°C for C11.

Unlike C10 and C11, we did not detect any relaxation process in the N* phase for the C12 compound. This continuous decrease of the amplitude of the relaxation mechanism in the N* phase, when passing from the C10 to the C11 compound and its disappearance for C12, is certainly connected with the proximity of a N*–SmA–SmC* multicritical point, which is closely related to the chain length. Indeed, for a longer chain homologue (C12), the temperature range of the SmA phase is relatively large and the N*–SmA–SmC* multicritical point is far enough from the atmospheric pressure condition to prevent any smectic fluctuations [20, 27]. These fluctuations become important in the N* phase for C10 and C11. This probably explains the lack of the relaxation process attributed to local smectic order in the N* phase for C12 material.

4. Conclusions

Ferroelectric liquid crystal materials exhibiting the N*-SmA-SmC* phase sequence have been studied by electro-optic and dielectric spectroscopy. From dielectric measurements without bias voltage, we have studied the soft mode in the SmA phase. Using the experimental data and a Landau model of the SmC*-SmA transition, we have estimated the soft-mode rotational viscosity and the electroclinic coefficient in the SmA phase.

High values of the electroclinic coefficient are found and its amplitude is connected to the ferroelectric polarisation in the SmC* phase via the piezoelectric coupling term. In the paraelectric phase, the soft-mode dielectric strength, the corresponding relaxation frequency and the electroclinic coefficient satisfy the Curie–Weiss law. In the N* phase, a dielectric relaxation mechanism at relatively high frequency was detected. This dielectric process was attributed to a soft-mode like mechanism and interpreted by the existence of local smectic order emphasised by the proximity of the SmC*-SmA-N* multicritical point for the compounds with shorter alkyloxy chains (C10 and C11). This mechanism was not observed for the C12 homologue with a longer chain.

References

[1] Garoff, S.; Meyer, R.B. *Phys. Rev. Lett.* **1977**, *38*, 848–851.
[2] Garoff, S.; Meyer, R.B. *Phys. Rev. A: At., Mol., Opt. Phys.* **1979**, *19*, 338–347.
[3] Andersson, G.; Dahl, I.; Kuczynski, W.; Lagerwall, S.T.; Skarp, K.; Stebler, B. *Ferroelectrics* **1984**, *84*, 285–315.
[4] Marcerou, J.P. *J. Phys. II* **1994**, *4*, 751–761.
[5] Nguyen, H.T.; Babeau, A.; Léon, C.; Marcerou, J.P.; Destrade, C.; Soldera, A.; Guillon, D.; Skoulios, A. *Liq. Cryst.* **1991**, *9*, 253–266.
[6] Marzec, M.; Dabrowski, R.; Fafara, A.; Haase, W.; Hiller, S.; Wrobel, S. *Ferroelectrics*, **1996**, *180*, 127–135.
[7] Etxebarria, J.; Zubia, J. *Phys. Rev. A: At., Mol., Opt. Phys.* **1991**, *44*, 6626–6631.

[8] Bahr, C.H.; Heppke, G. *Liq. Cryst.* **1987**, *2*, 825–831.
[9] Dupont, L.; Glogarova, M.; Marcerou, J.P.; Nguyen, H.T.; Destrade, C.; Lejcek, L. *J. Phys. II* **1991**, *1*, 831–844.
[10] Gouda, F.; Skarp, K.; Lagerwall, S.T. *Mol. Cryst. Liq. Cryst.* **1991**, *209*, 99–107.
[11] Manna, U.; Song, J.K.; Vij, J.K.; Naciri, J. *J. Appl. Phys. Lett*. **2009**, *94*, 012901–012903.
[12] Blinov, L.M.; Beresnev, L.A.; Haase, W. *Ferroelectrics* **1995**, *174*, 211–239.
[13] Komitov, L.; Lagerwall, S.T.; Stebler, B.; Andersson, G.; Flatischler, K. *Ferroelectrics* **1991**, *114*, 167–179.
[14] Lee, S.D.; Patel, J.S. *Phys. Rev. Lett. A* **1991**, *155*, 435–439.
[15] Legrand, C.; Isaert, N.; Hemine, J.; Buisine, J.M.; Parneix, J.P.; Nguyen, H.T.; Destrade, C. *Ferroelectrics* **1991**, *121*, 21–31.
[16] Biradar, A.M.; Bawa, S.S.; Saxena, K.; Chandra, S. *J. Phys. II* **1993**, *3*, 1787–1793.
[17] Li, Z.; Di Lisi, G.A.; Petschek, R.G.; Rosenblatt, C. *Phys. Rev. A: At., Mol., Opt. Phys.* **1990**, *41*, 1997–2004.
[18] Li, Z.; Ambigapathy, R.; Petschek, R.G.; Rosenblatt, C. *Phys. Rev. A: At., Mol., Opt. Phys.* **1991**, *43*, 7109–7112.
[19] Karlsson, M.; Komitov, L.; Lagerwall, S.T. *Jpn. J. Appl. Phys.* **1999**, *38*, 1470–1473.
[20] Legrand, C.; Isaert, N.; Hemine, J.; Buisine, J.M.; Parneix, J.P.; Nguyen, H.T.; Destrade, C. *J. Phys. II* **1992**, *2*, 1545–1562.
[21] Hemine, J.; Legrand, C.; Isaert, N.; Nguyen, H.T. *Liq. Cryst.* **2003**, *30*, 227–234.
[22] Clark, N.A.; Lagerwall, S.T. *Appl. Phys. Lett.* **1980**, *36*, 899–901.
[23] Petit, M.; Daoudi, A.; Ismaili, M.; Buisine, J.M. *Eur. Phys. J. E* **2006**, *20*, 327–333.
[24] Martinot Lagarde, Ph.; Duke, R.; Durand, G. *Mol. Cryst. Liq. Cryst*. **1981**, *75*, 249–286.
[25] Legrand, C.; Parneix, J.P. *J. Phys.* **1990**, *51*, 787–798.
[26] Cole, K.S.; Cole, R.H. *J. Chem. Phys.* **1941**, *9*, 341–351.
[27] Hemine, J.; Legrand, C.; Daoudi, A.; Isaert, N.; Nguyen, H.T. *Liq. Cryst.* **2007**, *34*, 241–249.
[28] Carlsson, T.; Zeks, B.; Levstik, A.; Filipic, C.; Levstik, I.; Blinc, R. *Phys. Rev. A: At., Mol., Opt. Phys.* **1990**, *42*, 877–889.
[29] Khened, S.M.; Prasad, S.K.; Shivkuma, B.; Sodashiva, B.K. *J. Phys. II* **1991**, *2*, 171–180.
[30] Petit, M.; Daoudi, A.; Ismaili, M.; Buisine, J.M. *Phys. Rev. E: Stat., Nonlinear, Soft Matter Phys.* **2006**, *74*, 061707–071714.
[31] Li, Z.; Rolfe, G.A.; Petschek, R.G.; Rosenblatt, C. *Phys. Rev. Lett.* **1989**, *62*, 796–799.